Blowing Model for Turbulent Boundary-Layer Dust Ingestion

Harold Mirels*
The Aerospace Corporation, El Segundo, California

The rate at which dust is ingested into a turbulent boundary layer is deduced for the case of a semi-infinite flat plate and for the boundary layer behind a moving shock wave. Conventional turbulent boundary-layer theory is used. It is assumed that the local dust-ingestion rate corresponds to the "blowing" rate at which the local unblown surface shear $C_{f,0}$ is reduced to a value $C_{f,t}$ that is just sufficient to maintain surface particles in a mobile state. It is further assumed that the particle-velocity equilibration distance ℓ_E is small compared with the local boundary-layer thickness δ. For $C_{f,0}/C_{f,t} \gg 1$, it is found that erosion rate and boundary-layer thickness parameters are weakly (logarithmically) dependent on $C_{f,0}/C_{f,t}$ and the maximum dust loading within the boundary layer is approximately equal to one. The theoretical predictions for local erosion rate, boundary thickness, and dust density are compared with the limited experimental results of Hartenbaum and Ausherman for the semi-infinite flat-plate and moving-shock cases, respectively. Agreement within about a factor of two is obtained, despite the fact that, for some of the data, the value of ℓ_E/δ was of order one. Further comparison with experiment is recommended.

Nomenclature

a = speed of sound, cm/s
B = blowing parameter, Eq. (1)
$C_{D,p}$ = particle drag coefficient, Eq. (24)
C_f = local shear coefficient
$C_{f,0}$ = shear coefficient in absence of blowing
$C_{f,t}$ = threshold shear coefficient, Eq. (3)
d = particle diameter, cm
F_D = drag force on particle
g = gravitation constant, cm/s^2
L = streamwise station, cm
ℓ_E = particle-velocity equilibration distance, cm
M = Mach number, u/a
$\dot{M}_p$ = net particle flux at station L, Eq. (5)
m = particle mass, g
n = velocity profile exponent, Eq. (7)
n_p = number of particles per unit volume
p = pressure, atm
Re_d = particle Reynolds number, $\rho_w v_{p,w} d/\mu_w$
Re_x = Reynolds number, $\rho_e u_e x/\mu_e$
$\bar{Re}_x$ = equivalent flat-plate Reynolds number, $\rho_e u_e (W-1)^2 x/\mu_e$
T = temperature
u,v = fluid velocity in x,y directions
u_p,v_p = particle velocity in x,y directions
u_τ = friction velocity, $(2\tau_w/\rho_w)^{1/2}$
W = density ratio across shock, ρ_e/ρ_1
x,y = streamwise and vertical directions, cm
δ = boundary-layer thickness
θ = boundary-layer momentum thickness
μ = viscosity, g/s·cm
ρ = fluid density, g/cm^3
ρ_p = particulate density, $n_p m$
σ = single-particle density, g/cm^3
τ_w = surface shear
ω = viscosity law exponent, Eq. (11)

Subscripts

e = external to boundary layer
p = particle value
t = threshold value, Eq. (2)
w = surface value
0 = nonblowing value
1 = upstream of shock wave

Received Oct. 4, 1983; revision received March 6, 1984.

*Head, Fluid Dynamics Department, Laboratory Operations.

Introduction

THE interaction of a turbulent wind with a dust-laden surface, and the subsequent lofting of dust particles, is of interest for a variety of applications.

If the surface particles are relatively heavy and the wind speed is not large, the individual particles ejected from the ground rise a certain distance, travel with the wind, and then descend back to the ground. This process, referred to as "saltation," leads to the generation of desert dunes.[1,2] The saltation region occurs in the range[2]

$$\mathcal{O}(10^{-2}) \leq \frac{F_D}{F_g} \equiv \frac{\rho u_\tau^2}{\sigma g d} \leq \mathcal{O}(1) \tag{1}$$

where F_D is the aerodynamic drag force on a particle resulting from turbulent fluid motion and F_g the gravitational force. Other symbols are defined in the Nomenclature. The lower limit is related to the minimum force required to loft a particle and the upper limit corresponds to the limit beyond which the particle goes into suspension. For sand particles in standard air, Eq. (1) becomes approximately $\mathcal{O}(10^4) \leq u_\tau^2/d \leq \mathcal{O}(10^6)$, where u_τ (cm/s) is the local friction velocity[2] (i.e., the characteristic turbulent eddy velocity near a wall) and d (cm) the particle diameter. For $d = 10^{-2}$ cm, the friction velocity is limited to values of 10-100 cm/s in order for saltation to occur.

With an increase in wind velocity, the dust particles enter suspension. This process is of interest in the generation of dust clouds and in the evaluation of nuclear weapons effects.[3] Relatively few experimental studies have been made of dust ingestion into a high-speed turbulent boundary layer. Hartenbaum[4] has investigated the airflow over a semi-infinite sand bed with freestream velocities in the range 3×10^3-10^4 cm/s and a mean particle diameter $d = 0.025$ cm. Ausherman[5] has investigated the turbulent boundary layer behind a shock moving over a sand bed with a mean particle diameter $d = 0.009$ cm. Flow velocities relative to the wall were in the range 2-5 $\times 10^4$ cm/s.

Current analytical models for estimating the local rate of surface erosion generally assume that the erosion rate is proportional to the surface shear that would exist in the absence of lofting (e.g., Refs. 6 and 7). The constant of proportionality is deduced from Hartenbaum's experimental results. The dependence of the constant of proportionality on particle and fluid properties is not known. Hence, the range of validity of this approach is uncertain with departure from Hartenbaum's test conditions.

The present study is an attempt to evaluate local erosion rates using conventional turbulent boundary-layer theory. The case considered is one wherein the supply of surface particles is unlimited and the particles reach velocity equilibration with the ambient fluid soon after their injection into the boundary layer. The flow is then similar to the case of a turbulent boundary layer with surface blowing.[8-10] It is assumed that the blowing rate is such that the surface shear is reduced to the threshold value of the shear at which surface-particle mobility is maintained. A similar approximation was made for the saltation regime in Ref. 2. The theory is described in the next section. Turbulent-layer properties are deduced for a flow of air over a semi-infinite sand bed and for the boundary layer behind a shock moving over a sand bed. Comparisons are made with the experimental observations of Hartenbaum[4] and Ausherman.[5]

Theory

Integral relations for a turbulent boundary layer, with blowing, are noted. They are solved subject to the assumption that the wall shear equals the threshold value at which surface-particle mobility is maintained. Expressions are derived for the rate of dust ingestion into a turbulent boundary on a flat plate and behind a moving shock wave (e.g., Fig. 1).

Boundary-Layer Equations

Consider a turbulent boundary layer with surface blowing and zero pressure gradient. The effect of blowing on the local shear and boundary layer thickness can be approximated by

$$\frac{C_f}{C_{f,0}} = \frac{\ell n(1+B)}{B} \tag{2a}$$

and

$$\frac{\delta}{\delta_0} = \frac{1+B}{B}\,\ell n(1+B) \tag{2b}$$

where

$$B \equiv \frac{2}{C_f}\,\frac{(\rho_p v_p)_w}{\rho_e u_e} \tag{2c}$$

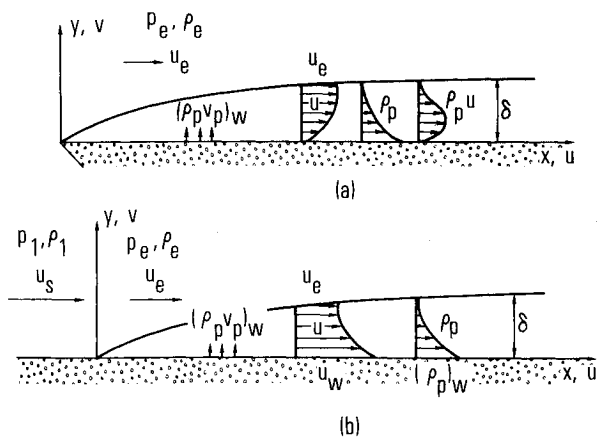

Fig. 1 Flowfields and coordinate systems for studying the ingestion of dust into a turbulent boundary layer: a) semi-infinite flat plate, b) boundary layer behind a moving shock in a shock-stationary coordinate system ($u_w = u_s$).

where subscript zero denotes nonblowing values and $(\rho_p v_p)_w$ the local rate at which particles are ingested into the boundary layer. Other symbols are defined in the Nomenclature. The form of Eq. (2a) can be deduced from a consideration of Couette flow with blowing[8] and has been confirmed experimentally[8] for values of the blowing parameter B up to about 20. Equation (2b) is deduced from the momentum integral equation under the assumption that the ratio θ/δ is relatively independent of blowing.[9] Equation (2b) is less well established than Eq. (2a).

Threshold Shear

The lowest value of surface shear at which surface-particle mobility is maintained is termed threshold shear τ_t and can be expressed by

$$\tau_t = \beta \sigma g d \tag{3a}$$

where β is a dimensionless constant that can be taken equal to[1,2]

$$\beta = 0.0064 \tag{3b}$$

The constant β may be viewed as the ratio of shear force $\tau_t d^2$ to the gravitational force $\sigma g d^3$ at which surface-particle motion can be maintained.

Dust-Ingestion Equations

We now assume turbulent flow over a surface consisting of an unlimited number of small particles, and also that the local rate of ingestion of particles into the boundary layer is just sufficient to reduce the local surface shear to the threshold value. Thus,

$$C_f = C_{f,t} \equiv 2\tau_t / \rho_e u_e^2 \tag{4}$$

This assumption is similar to one made in Ref. 2—that, in effect, small departures of C_f from $C_{f,t}$ result in a relatively large blowing rate. Hence, the local blowing rate corresponds to the value needed to reduce the unblown shear $C_{f,0}$ to a value of order $C_{f,t}$. Also, as will be seen, $B \gg 1$ for cases of practical interest. For these cases, the local blowing rate parameter $(\rho_p v_p)_w/\rho_e u_e$ depends on the log of C_f. Hence, small departures of C_f from $C_{f,t}$ should not significantly affect the result and Eq. (4) is applicable.

If the surface shear in the absence of blowing $C_{f,0}$ is known, the local blowing parameter B can be found from Eqs. (2a) and (4) by iteration, namely

$$B = (C_{f,0}/C_{f,t})\,\ell n(1+B) \tag{5a}$$

The local blowing rate is then

$$\frac{(\rho_p v_p)_w}{\rho_e u_e} = \frac{C_{f,t} B}{2} = \frac{C_{f,0}}{2}\,\ell n(1+B) \tag{5b}$$

and is seen to depend only weakly on B. Other boundary-layer properties are found as follows. The net particle flux at streamwise station $x = L$ can be expressed in the alternative forms

$$\dot{M}_p = \int_0^L (\rho_p v_p)_w dx \tag{6a}$$

$$= \int_0^\delta (\rho_p u)_L dy \tag{6b}$$

Equation (6b) assumes velocity equilibration between the particles and the local flow. It will be shown that for the

present applications, $C_{f,0} \sim x^{-1/5}$. If the weak dependence of $\ell n(1+B)$ on x is ignored, Eq. (6a) becomes

$$\frac{\dot{M}_p}{\rho_e u_e \delta_0} = \frac{5}{8}\frac{xC_{f,0}}{\delta_0}\ell n(1+B) \tag{7}$$

where all variables are evaluated at $x=L$. In order to evaluate Eq. (6b), we assume

$$\frac{u}{u_e} = 1 - \frac{\rho_p}{(\rho_p)_w} = \left(\frac{y}{\delta}\right)^{1/n} \tag{8}$$

That is, it is assumed that normalized streamwise velocity and particle-density profiles are similar and have a power law variation with y/δ. Substitution into Eq. (6b) yields

$$\frac{\dot{M}_p}{(\rho_p)_w u_e \delta} \equiv \frac{\theta}{\delta} = \frac{n}{(1+n)(2+n)} \tag{9a}$$

$$= \frac{7}{72} \qquad (n=7) \tag{9b}$$

Equation (9a) is relatively insensitive to n and the value of $n=7$ will be used. Equations (2b), (7), and (9) yield the particle density at the wall, namely,

$$\frac{(\rho_p)_w}{\rho_e} = \frac{45}{7}\frac{xC_{f,0}}{\delta_0}\frac{B}{1+B} \tag{10a}$$

and the particle density profile

$$\frac{\rho_p}{\rho_e} = \left[1 - \left(\frac{y}{\delta}\right)^{1/7}\right]\frac{(\rho_p)_w}{\rho_e} \tag{10b}$$

The particle velocity at the wall is, from Eqs. (2b), (5b), and (10a),

$$\frac{(v_p)_w}{u_e} = \frac{7}{90}\frac{\delta}{x} \tag{10c}$$

These equations are now evaluated for the case of incompressible flow over a flat plate and for flow behind a moving shock wave.

Incompresssible Flow over a Flat Plate

Consider incompressible flow over a flat plate (Fig. 1a). In the absence of blowing and ignoring surface roughness effects,[11]

$$\frac{1}{0.0296}\frac{C_{f,0}}{2} = \frac{1}{0.37}\frac{\delta_0}{x} = \left(\frac{\mu_e}{\rho_e u_e x}\right)^{1/5} \tag{11a}$$

Further, consider air at near-standard temperature ($T_e = 290$ K). The following numerical values then apply:

$$(T_e/290)(\rho_e/p_e) = 1.218\times10^{-3}\ \text{g/cm}^3\cdot\text{atm} \tag{12a}$$

$$(290/T_e)^{1/2} a_e = 3.415\times10^{4}\ \text{cm/s} \tag{12b}$$

$$(290/T_e)^{\omega}\mu_e = 1.829\times10^{-4}\ \text{g/s}\cdot\text{cm} \tag{12c}$$

where $\omega = 0.7$. For sand-like particles

$$\beta = 0.0064 \qquad d \doteq 10^{-2}\ \text{cm} \tag{12d}$$

$$\sigma \doteq 2.5\ \text{g/cm}^3 \qquad g = 980\ \text{cm/s}^2 \tag{12e}$$

The expressions for unblown and threshold shear become

$$\left(\frac{290}{T_e}\right)^{0.24}(M_e p_e x)^{1/5} C_{f,0} = 5.023\times10^{-3} \tag{13a}$$

$$\left(\frac{290}{T_e}\right)^{0.24}\frac{(M_e p_e x)^{1/5}}{M_e^2 p_e}\frac{C_{f,0}}{C_{f,t}} = \frac{2.275\times10^{4}}{\beta d/(6.4\times10^{-5})} \tag{13b}$$

where p_e and x are in atmospheres and centimeters, respectively, and the dependence on βd is displayed. Boundary-layer properties are found from

$$\frac{C_{f,0}}{C_{f,t}} = \frac{B}{\ell n(1+B)} \tag{14a}$$

$$\left(\frac{290}{T_e}\right)^{0.24}\frac{(M_e p_e x)^{1/5}}{2.511\times10^{-3}}\frac{(\rho_p v_p)_w}{\rho_e u_e} = \ell n(1+B) \tag{14b}$$

$$\frac{(M_e p_e x)^{1/5}}{3.139\times10^{-2}}\frac{\delta}{x} = \frac{1+B}{B}\ell n(1+B) \tag{14c}$$

$$\frac{1}{1.03}\frac{(\rho_p)_w}{\rho_e} = \frac{B}{1+B} \tag{14d}$$

These results are applicable for Reynolds numbers beyond the transition value, $Re_x \gtrsim 10^6$. Thus, for air, the region of applicability is

$$(290/T_e)^{1.2}(M_e p_e x) \gtrsim 4.4 \tag{14e}$$

The variation of boundary-layer properties with increase in $C_{f,0}/C_{f,t}$ is indicated in Table 1 and Fig. 2. For the large values of $C_{f,0}/C_{f,t}$ of present interest

$$\ell n(1+B) \equiv \frac{B}{C_{f,0}/C_{f,t}} = \left(\ell n\frac{C_{f,0}}{C_{f,t}}\right)\left\{1 + \mathcal{O}\left[\frac{\ell n[\ell n(C_{f,0}/C_{f,t})]}{\ell n(C_{f,0}/C_{f,t})}\right]\right\} \tag{15}$$

Substituting Eq. (15) into Eq. (14) provides an explicit solution for boundary-layer variables in terms of the parameter $C_{f,0}/C_{f,t}$. In this region, the local blowing rate parameter $(\rho_p v_p)_w/\rho_e u_e$ and the boundary-layer thickness parameter δ/x have a weak (logarithmic) dependence on $C_{f,0}/C_{f,t}$, as may be observed in Fig. 2. This result is consistent with the previous approximation that the shear can be

Table 1 Corresponding values of blowing parameters and shear ratio $C_{f,0}/C_{f,t}$

$\frac{C_{f,0}}{C_{f,t}}$	B	$\ell n(1+B)$	$\frac{1+B}{B}\ell n(1+B)$	$\frac{B}{1+B}$
1.05×10^{0}	10^{-1}	9.53×10^{-2}	1.05×10^{0}	9.09×10^{-2}
1.44×10^{0}	10^{0}	6.93×10^{-1}	1.39×10^{0}	5.00×10^{-1}
4.17×10^{0}	10^{1}	2.40×10^{0}	2.64×10^{0}	9.09×10^{-1}
2.17×10^{1}	10^{2}	4.62×10^{0}	4.66×10^{0}	9.90×10^{-1}
1.45×10^{2}	10^{3}	6.91×10^{0}	6.92×10^{0}	9.99×10^{-1}
1.09×10^{3}	10^{4}	9.21×10^{0}	9.21×10^{0}	1.00×10^{0}
8.69×10^{3}	10^{5}	1.15×10^{1}	1.15×10^{1}	1.00×10^{0}
7.24×10^{4}	10^{6}	1.38×10^{1}	1.38×10^{1}	1.00×10^{0}

Table 2 Comparison with the Hartenbaum[4] experimental study of airflow over a semi-infinite sand bed[a]

		Theory									Experiment		
u_e, ft/s	M_e	$\frac{C_{f,0}}{C_{f,t}}\times 10^{-1}$	$B\times 10^{-2}$	Re_d	$\frac{\ell_E}{\delta}$	$\frac{\delta}{\delta_0}$	$\frac{\delta}{x}\times 10^2$	$\frac{(\rho_p)_w}{\rho_e}$	$\frac{(\rho_p v_p)_w}{\rho_e u_e}\times 10^2$	$\frac{\delta}{x}\times 10^2$	$\frac{(\rho_p)_w}{\rho_e}$	$\frac{(\rho_p v_p)_w}{\rho_e u_e}\times 10^2$
111.8	0.0998	4.17	2.26	3.6	0.26	5.45	7.89	1.03	0.626	4.0	~2[b]	1.6
237.8	0.2123	16.22	11.42	8.4	0.55	7.05	8.78	1.03	0.669	5.0	~2.5	1.8
376.3	0.3360	37.07	29.64	13.8	0.87	8.00	9.08	1.03	0.724	7.0	~3	1.9

[a] Data taken at $x=488$ cm, Ottawa silica sand, $d=0.025$ cm, $T_e=290$ K, $p_e=1$ atm. [b] ~ denotes extrapolated value; ℓ_E/δ estimated from Eq. (28a).

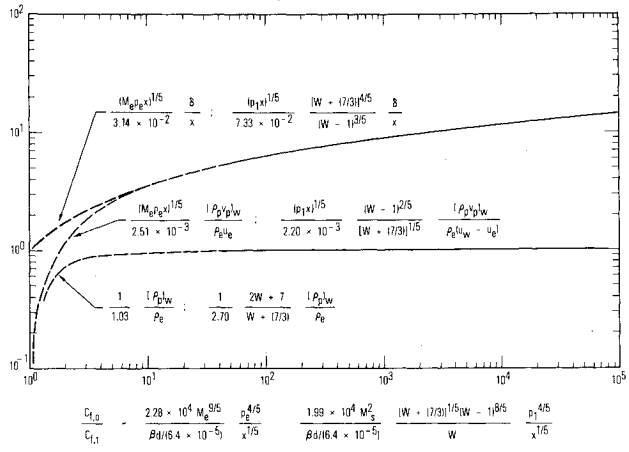

Fig. 2 Variation of turbulent boundary-layer properties with variation in $C_{f,0}/C_{f,t}$ for semi-infinite flat-plate and moving-shock cases (air, $T_1=290$ K, $p=$ atm, $x=$ cm).

assumed to be reduced by blowing to the threshold value for surface mobility.

For the present case of incompressible flow, $\rho_w=\rho_e$. The dust loading at the wall, $(\rho_p)_w/\rho_w$, is approximately equal to 1.03 for $C_{f,0}/C_{f,t}\geq 10$. The wall value of dust loading provides an upper bound on the dust loading within the boundary layer. The near-constant value of $(\rho_p)_w/\rho_w$ for $C_{f,0}/C_{f,t}>10$ is a reflection of the fact that the blowing rate and boundary-layer thickness grow at the same rate with the increase in $C_{f,0}/C_{f,t}$.

It has been assumed in the present model that the particles remain in suspension. The saltation-layer study by Owen[2] [e.g., Eq. (1)] suggests that this assumption may become invalid when $C_{f,0}/C_{f,t}\leq \mathcal{O}(100)$ and $B\leq \mathcal{O}(10^3)$. However, as will be shown, the results of Hartenbaum in Table 2 and Fig. 3a include data at $C_{f,0}/C_{f,t}=41.7$ that are consistent with the present model. Hence, the lower limit on $C_{f,0}/C_{f,t}$, for which the present results are useful, is not clear. The curves in Fig. 2 are dashed for $C_{f,0}/C_{f,t}<50$ to reflect the uncertainty in the lower limit of the suspension regime.

Boundary Layer behind a Moving Shock

The boundary layer behind a moving shock is illustrated in Fig. 1b. A shock-fixed coordinate system is used. In this coordinate system, the wall has a velocity u_w equal to the upstream flow velocity u_s. Flow properties up- and downstream of the shock are denoted by subscripts 1 and e, respectively. Boundary-layer parameters are normalized by the freestream velocity relative to the wall, u_w-u_e. Thus

$$C_{f,0}=2\tau_{w,0}/[\rho_e(u_w-u_e)^2] \tag{16a}$$

$$C_{f,t}=2\tau_t/[\rho_e(u_w-u_e)^2] \tag{16b}$$

$$B=\frac{2}{C_{f,t}}\frac{(\rho_p v_p)_w}{\rho_e(u_w-u_e)} \tag{16c}$$

The normalized velocity and particle-density profiles are

$$\frac{u_w-u}{u_w-u_e}=1-\frac{\rho_p}{(\rho_p)_w}=\left(\frac{y}{\delta}\right)^{1/n} \tag{17}$$

The net particle flux at $x=L$ is [assuming $C_{f,0}\sim x^{-1/5}$ and neglecting the dependence of $\ell n(1+B)$ on x]

$$\frac{\dot{M}_p}{\rho_e(u_w-u_e)\delta}=\frac{5}{8}\frac{xC_{f,0}}{\delta_0}\frac{B}{1+B} \tag{18a}$$

or, alternately, for $n=7$,

$$\frac{\dot{M}_p}{(\rho_p)_w(u_w-u_e)\delta}=\frac{2W+7}{72(W-1)} \tag{18b}$$

where $W=(\rho_e/\rho_1)=u_w/u_e$. The particle density and velocity at the wall are, respectively,

$$\frac{(\rho_p)_w}{\rho_e}=\frac{5}{8}\frac{72(W-1)}{2W+7}\frac{xC_{f,0}}{\delta_0}\frac{B}{1+B} \tag{19a}$$

and [from Eqs. (2b), (16c), and (19a)]

$$\frac{(v_p)_w}{u_w-u_e}=\frac{4}{5}\frac{2W+7}{72(W-1)}\frac{\delta}{x} \tag{19b}$$

In the absence of blowing, the turbulent boundary-layer properties can be expressed (for air with $T_1\approx 290$ K and sand-like particles) as[10]

$$(p_1x)^{1/5}C_{f,0}=4.397\times 10^{-3}\frac{[W+(7/3)]^{1/5}}{(W-1)^{2/5}} \tag{20a}$$

$$\frac{xC_{f,0}}{\delta_0}=0.0600\frac{W+(7/3)}{W-1} \tag{20b}$$

$$\frac{(p_1x)^{1/5}}{p_1M_s^2}\frac{C_{f,0}}{C_{f,t}}=\frac{1.991\times 10^4}{\beta d/(6.4\times 10^{-5})}\frac{[W+(7/3)]^{1/5}(W-1)^{8/5}}{W} \tag{20c}$$

The solution, with dust ingestion, is then found from

$$\frac{C_{f,0}}{C_{f,t}}=\frac{B}{\ell n(1+B)} \tag{21a}$$

$$\frac{(p_1x)^{1/5}}{2.198\times 10^{-3}}\left(\frac{(W-1)^2}{W+(7/3)}\right)^{1/5}\frac{(\rho_p v_p)_w}{\rho_e(u_w-u_e)}=\ell n(1+B) \tag{21b}$$

Table 3 Comparison with the Ausherman[5] experimental study of a turbulent boundary layer behind a shock moving over a sand bed[a]

			Theory								Experiment	
M_s	W	x, cm	$\frac{C_{f,0}}{C_{f,t}}\times 10^{-4}$	$B\times 10^{-5}$	$Re_d\times 10^{-1}$	$\frac{\ell_E}{\delta}$	$\frac{\delta}{x}\times 10$	$\frac{(\rho_p)_w}{\rho_e}$	$\frac{(\rho_p v_p)_w}{\rho_e(u_w-u_e)}\times 10^2$	$\frac{\delta}{x}\times 10$	$\frac{(\rho_p)_w}{\rho_e}$
1.41	1.71	30.5	1.00	1.16	4.8	3.3	1.15	1.05	1.96	0.36	~0.8[b]
		61.0	0.87	1.00	4.2	1.9	0.99	1.05	1.69	0.36	~1.1
		91.4	0.80	0.91	3.8	1.4	0.90	1.05	1.54	0.36	~1.4
1.74	2.27	30.5	2.97	3.82	10.4	1.5	1.62	1.08	1.76	0.63	~0.4
		61.0	2.59	3.29	8.9	0.9	1.39	1.08	1.51	0.63	~0.7
		91.4	2.39	3.01	8.2	0.6	1.28	1.08	1.39	0.63	~1.0
2.25	3.02	15.2	9.29	13.09	30.2	1.2	2.38	1.11	1.90	1.0	~0.3
		30.5	8.09	11.27	26.0	0.7	2.05	1.11	1.63	1.0	~0.6
		45.7	7.46	10.33	23.9	0.5	1.88	1.11	1.50	1.0	~0.9

[a] Ottawa ultrafine sand, $d=0.009$ cm, $T_1=290$ K, $p_1=1$ atm. [b] ~denotes extrapolated value; ℓ_E/δ estimated from Eq. (27) with $C_{D,p}=1$.

$$\frac{(p_1 x)^{1/5}}{7.328\times 10^{-2}}\frac{[W+(7/3)]^{4/5}}{(W-1)^{3/5}}\frac{\delta}{x}=\frac{1+B}{B}\ell n(1+B) \tag{21c}$$

$$\frac{1}{2.70}\frac{2W+7}{W+(7/3)}\frac{(\rho_p)_w}{\rho_e}=\frac{B}{1+B} \tag{21d}$$

In order to insure that the boundary layer is turbulent, we require the equivalent flat-plate Reynolds number[10] to be in the range $\bar{R}e_x\equiv\rho_e u_e(W-1)^2 x/\mu_e\gtrsim 10^6$ or, for air,

$$\left(\frac{\mu_1}{\mu_e}\right)\left(\frac{290}{T_1}\right)^{1.2}(M_s p_1 x)(W-1)^2\gtrsim 4.4 \tag{22}$$

Equations (21) are identical in form with Eqs. (14) and are included in Fig. 2. The weak logarithmic dependence of the blowing rate and boundary-layer thickness parameters on $C_{f,0}/C_{f,t}$ is again observed. For $B\to\infty$ and $1\le W\le 10$, the particle density at the wall is in the narrow range $1.00\le(\rho_p)_w/\rho_e\le 1.23$. Evaluation of the dust loading at the wall, $(\rho_p)_w/\rho_w$, is more complex than for the previous flat-plate case. If we assume that the wall remains at its initial temperature, $T_w=T_1$, ideal-gas relations indicate

$$\frac{\rho_w}{\rho_1}=\frac{p_e}{p_1}=\frac{7M_s^2-1}{6}\qquad\text{(ideal air)} \tag{23}$$

The dust loading at the wall, for ideal air, is then

$$\frac{(\rho_p)_w}{\rho_w}=2.70\frac{W+(7/3)}{2W+7}\frac{6W}{7M_s^2-1}\frac{B}{1+B} \tag{24}$$

For strong shocks, $(\rho_p)_w/\rho_w$ falls below one. This is due to the fact that for strong shocks the air density at the wall rises more rapidly with shock strength than does the particle density at the wall. In these cases, the peak dust loading $(\rho_p)/\rho$ occurs within the interior of the boundary layer. However, this feature of the solution may be an artifact of the simplified particle-density profile assumed herein [Eq. (17)].

Velocity Equilibration

It has been assumed that the particles ingested into the boundary layer rapidly achieve velocity equilibration with the local flow. The region of validity of this assumption is now established.

Assume that the dust particles leave the surface vertically, with a velocity $v_{p,w}$. The initial value of drag coefficient is, for spherical particles,

$$C_{D,p}\doteq\frac{F_D}{[(1/2)\rho_w v_{p,w}^2][\pi(d/2)^2]} \tag{25a}$$

$$=\frac{24}{Re_d}\qquad Re_d\lesssim 10 \tag{25b}$$

$$=\mathcal{O}(1)\qquad Re_d\gtrsim 10 \tag{25c}$$

where

$$Re_d=(\rho_w v_{p,w} d)/\mu_w$$

where ρ_w and μ_w are fluid properties evaluated at the wall and Eq. (25b) corresponds to Stokes' drag law. Let t_E denote the time for the particle to reach velocity equilibration with the local fluid and ℓ_E the vertical distance from the wall at which velocity equilibration is reached. Approximate values for these quantities are

$$t_E=\frac{\ell_E}{v_{p,w}}=\left(\frac{v_p}{dv_p/dt}\right)_w \tag{26}$$

where $(dv_p/dt)_w=F_D/m$. For spherical particles

$$\frac{x}{d}\frac{\ell_E}{\delta}=\frac{4}{3}\frac{\sigma}{\rho_w C_{D,p}}\frac{x}{\delta} \tag{27}$$

In the Stokes region, $Re_d\lesssim 10$,

$$\frac{1}{2.02\times 10^4}\frac{x}{d}\frac{\ell_E}{\delta}=M_e\Phi\qquad\text{(plate)} \tag{28a}$$

$$=M_s\frac{2W+7}{7W}\Phi\qquad\text{(shock)} \tag{28b}$$

where

$$\Phi=\frac{\sigma d}{2.5\times 10^{-2}}\left(\frac{290}{T_1}\right)^{0.2} \tag{28c}$$

The quantity Φ equals one for $T_1=290$ K, $d=10^{-2}$ cm, and $\sigma=2.5$ g/cm^3. For $Re_d\gtrsim 10$, Eq. (27) is evaluated by assuming $C_{D,p}\doteq 1$. In this case, $\rho_w=\rho_e$ for a flat plate and ρ_w is evaluated from Eq. (23) for a moving shock.

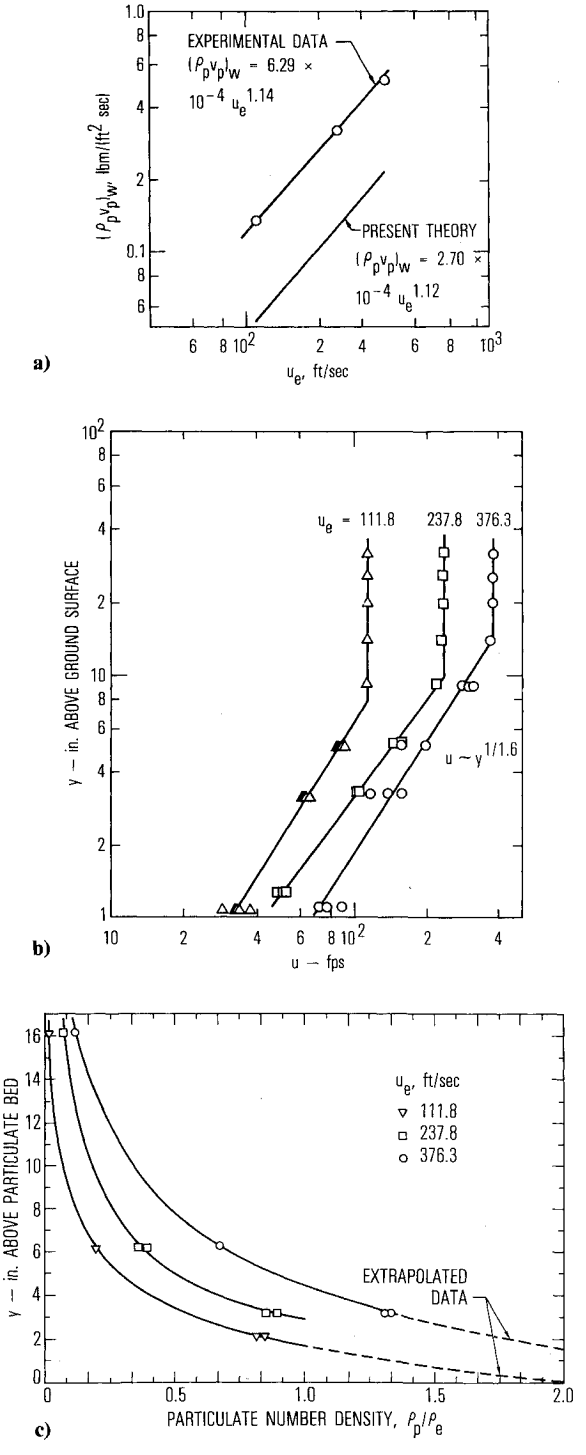

Fig. 3 Experimental data at $x = 488$ cm for a turbulent air boundary layer over a semi-infinite silica sand bed ($d = 0.025$ cm, $p_e = 1$ atm, $T_e = 290$ K, from Ref. 4): a) local mass erosion rate, b) wind velocity profile with particulate lofting, c) particulate number-density profile, ρ_p/ρ_e.

The assumption of rapid equilibration is valid when

$$\ell_E/\delta \ll 1 \tag{29}$$

which can be estimated by using Eqs. (27) and (28). For a given flow, the assumption of equilibration becomes more valid as x (and therefore δ) increases.

Equation (26) neglects the effect of cross flow on ℓ_E/δ. This neglect is valid in the Stokes flow regime but results in an overestimate of ℓ_E/δ for $Re_d \gtrsim 10$ (Ref. 12). The latter estimate is believed adequate for the present purposes.

Discussion

Dust ingestion into a turbulent boundary layer on a semi-infinite flat plate and behind a moving shock has been studied experimentally in Refs. 4 and 5, respectively. These experimental results are compared herein with the predictions of the present theory.

Flat Plate

Hartenbaum has reported[4] boundary-layer properties and dust-erosion rates at a distance of $x = 488$ cm downstream of the leading edge of a silica sand bed. The mean particle diameter was $d = 0.025$ cm and the test gas was air at standard conditions. Three freestream velocities ($M_e = 0.100$, 0.212, and 0.336) were considered. His results are indicated in Fig. 3 and Table 2. The predictions of the present theory are included in Table 2 and Fig. 3a.

The local erosion rate was correlated by Hartenbaum in the form (Fig. 3a)

$$(\rho_p v_p)_w = 6.29 \times 10^{-4} u_e^{1.14} \quad (\text{lbm/ft}^2 \cdot \text{s}) \tag{30a}$$

where u_e is in feet/second. For the range of flow conditions in Ref. 4, the present theory gives

$$(\rho_p v_p)_w = 2.70 \times 10^{-4} u_e^{1.12} \quad (\text{lbm/ft}^2 \cdot \text{s}) \tag{30b}$$

The present theory underestimates the local erosion rate by a factor of 0.4. The exponential dependence on u_e is remarkably close. It should be noted, however, that Eq. (30b) represents a tangent to the corresponding curve in Fig. 2 and therefore is applicable only for a limited range of u_e and x.

Local experimental boundary-layer thickness can be estimated from the velocity profiles in Fig. 3b and is included in Table 2. The predicted boundary-layer thickness is larger than the experimental value by a factor that varies from 2.0 to 1.3 as M_e increases from 0.100 to 0.336. The experimental value of δ, however, is not a well-defined quantity. The edge of the dust layer (see Fig. 2c) appears to extend to values of y that are greater than the experimental values of δ inferred from the velocity profiles in Fig. 2b and are in better agreement with present boundary-layer thickness predictions. The experimental velocity profile in Fig. 3b indicates a power law $u \sim y^{1/n}$ with $n = 1.6$, as opposed to the value $n = 7$ used herein. The reduction in n, with an increase in blowing rate, is physically realistic. The present theory can be generalized to consider velocity profiles of the form $y^{1/n}$, but the extension does not appear warranted at the present time.

The dust density profiles presented in Ref. 4 have been extrapolated to the wall in order to provide a rough estimate of $(\rho_p)_w/\rho_e$. Values of 2-3 are inferred. These are in approximate agreement with the predicted value of 1.03.

The theoretical estimate for the parameter ℓ_E/δ increases from 0.3 to 0.9 as M_e increases from 0.100 to 0.336. Hence, the applicability of the theory at the larger values of M_e may be questioned. However, in view of the fact that no attempt was made to adjust the single free parameter in the present study (β), the agreement between theory and experiment is surprisingly good. The experimental and theoretical predictions of local erosion rate, boundary-layer thickness, and dust density near the wall agree to within about a factor of two. No systematic divergence between theory and experiment is noted as ℓ_E/δ increases from 0.3 to 0.8. This suggests that the present theory may be applicable in the extended range $\ell_E/\delta \lesssim 1.0$, as defined herein, to within an accuracy of about a factor of two.

Boundary Layer behind a Moving Shock

Ausherman[5] has measured the turbulent boundary layer behind a shock moving over a silica dust bed. The mean particle size was $d = 0.9 \times 10^{-2}$ cm. Measurements were made at a fixed station, as a function of time after shock arrival, for

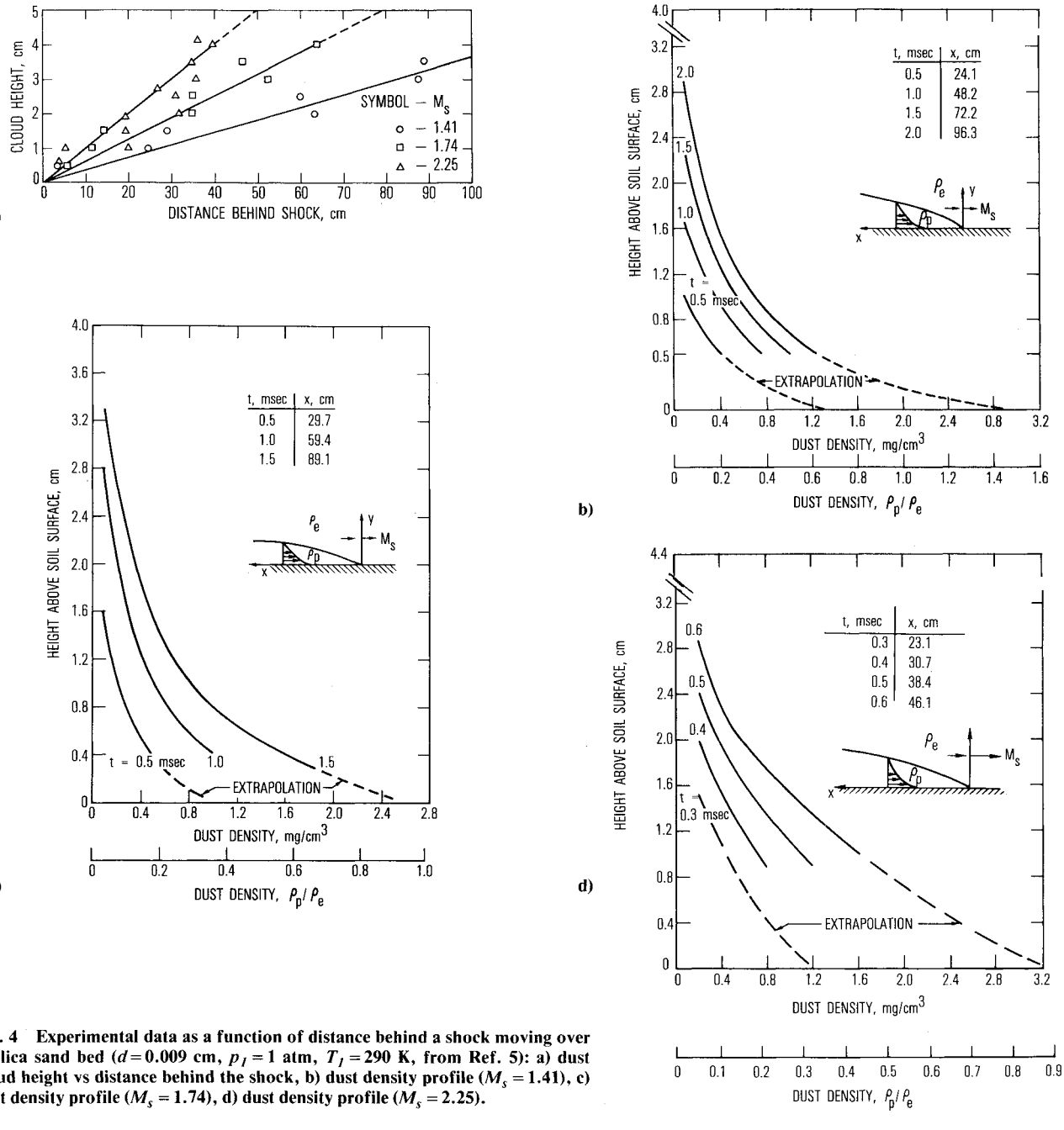

Fig. 4 Experimental data as a function of distance behind a shock moving over a silica sand bed ($d = 0.009$ cm, $p_1 = 1$ atm, $T_1 = 290$ K, from Ref. 5): a) dust cloud height vs distance behind the shock, b) dust density profile ($M_s = 1.41$), c) dust density profile ($M_s = 1.74$), d) dust density profile ($M_s = 2.25$).

shocks moving into standard air at $M_s = 1.4.$, 1.74, and 2.25. Time after shock arrival and distance behind the shock are related by $t = x/u_s$. The variation of dust cloud height with time was evaluated by observing the time at which optical extinction commenced at each of four vertical test positions. The results are given in Fig. 4a. The variation of dust density with height is indicated in Figs. 4b-4d as a function of time after shock arrival and shock Mach number. The experimental results are compared with theoretical predictions in Table 3.

Comparison of the theoretical and experimental estimates for dust cloud height indicates that the theory overpredicts the height by factors that range from 3.2 to 1.9 for the data in Table 3. The discrepancy is reduced with an increase in x and M_s. The magnitude of the overprediction is about the same as for the flat-plate case.

The dust density profiles were extrapolated to provide estimates of the dust density near the wall. The extrapolated values are in approximate agreement (to within about a factor of two) with the theoretical predictions.

Values of Re_d and ℓ_E/δ are included in Table 4. The latter has been calculated from Eq. (27) by using $C_{D,p} = 1$. It is seen that ℓ_E/δ ranges in value from 3.3 to 0.50, with the lower values corresponding to increased M_s and x. These values of ℓ_E/δ, however, are believed to be over estimates due to the neglect of cross flow in the non-Stokes regime.[12] The agreement between theory and experiment appears again to be within about a factor of two for those cases where $\ell_E/\delta \lesssim 1$.

Conclusion

The present theory contains a number of critical assumptions. The most important are that 1) conventional turbulent boundary-layer correlations apply for very large values of the blowing parameter B, and 2) the effect of dust ingestion is to reduce the wall shear to the threshold value needed to maintain surface-particle mobility. In addition, it has been assumed that the local blowing rate is not particle limited and that the particles are in local velocity equilibration with the

ambient fluid. Simple normalized profiles were assumed in order to calculate dust loading.

The theory contains a single free numerical parameter β, which was taken to equal the value recommended by Owen in his study of the saltation process.[2] It is somewhat remarkable that the predicted erosion rates and boundary-layer thicknesses agreed to within about a factor of two with the experimental results of Hartenbaum[4] and Ausherman.[5] This agreement may be fortuitous since the amount of experimental data is meager and some of the data (particularly Ausherman's) violates the assumption $\ell_E/\delta \ll 1$.

A major result of the present study is that for $C_{f,0}/C_{f,t} \gg 1$, the boundary-layer parameters have a logarithmic dependence in $C_{f,0}/C_{f,t}$ and, hence, are only weakly dependent on the latter parameter. This should simplify the estimate of local erosion rates in the flows of interest. However, further confirmation of the present theory is needed.

Acknowledgment

This work was partially supported by the Defense Nuclear Agency under U.S. Air Force Space Division Contract FO4701-82-C-0083.

References

[1] Bagnold, R. A. *The Physics of Blown Sands and Desert Dunes,* Methuen and Co., Ltd., London, 1941.

[2] Owen, P. R., "Saltation of Uniform Grains in Air," *Journal of Fluid Mechanics,* Vol. 20, Pt. 2, 1964, pp. 225-242.

[3] Ullrich, G. W., "Simulation of Dust-Laden Flow Fields," Paper presented at Seventh International Symposium, Military Applications of Blast Simulation, Medicine Hat, Canada, June 13-27, 1981.

[4] Hartenbaum, B., "Lofting of Particulates by a High-Speed Wind," Defense Nuclear Agency, Rept. 2737, Sept. 1971.

[5] Ausherman, D. R., "Initial Dust Lofting: Shock-Tube Experiments," Defense Nuclear Agency, Rept. 3162F, Sept. 1973.

[6] Kirsch, J. W., "Near-Surface Nuclear Dust Cloud Studies," Defense Nuclear Agency, Rept. 4332F, Jan. 1977.

[7] Barthel, J. R., "Dust Modeling Update," S-Cubed Corp., unpublished report, Dec. 1982.

[8] Dorrance, W. H., *Viscous Hypersonic Flow,* McGraw-Hill Book Co., New York, 1962, pp. 59, 206-220.

[9] Kays, W. M. and Moffat, R. J., "The Behavior of Transpired Turbulent Boundary Layers," *Studies in Convection,* edited by B. E. Launder, Academic Press, New York, 1975, p. 251.

[10] Mirels, H., "Turbulent Boundary Layer Behind Constant Velocity Shock Including Wall Blowing Effects," *AIAA Journal,* Vol. 22, Aug. 1984, pp. 1042-1047.

[11] Schlichting, H., *Boundary Layer Theory,* McGraw-Hill Book Co., New York, 1960, pp. 16, 485, and 537.

[12] Rudinger, G., "Penetration of Particles Injected into a Constant Cross Flow," *AIAA Journal,* Vol. 12, Aug. 1974, pp. 1138-1140.